

Elastic properties and freezing of argon confined in mesoporous glass

Klaus Schappert* and Rolf Pelster†

FR 7.2 Experimentalphysik, Universität des Saarlandes, 66123 Saarbrücken, Germany

(Received 24 July 2008; revised manuscript received 2 October 2008; published 13 November 2008)

We study the elastic properties of argon confined in mesoporous Vycor glass with a mean pore diameter of 8 nm. For this purpose volumetric adsorption and desorption measurements are combined with simultaneous ultrasonic measurements. Therewith we obtain the effective shear modulus as a function of the pore filling reflecting both the spatial arrangement and the freezing process of confined argon. Below the freezing point of argon the adsorption process proceeds in three steps. (I) The first adsorbed layers of argon do not contribute to the measured shear modulus, i.e., they do not behave like a solid. (II) In an intermediate range of pore filling the shear modulus increases linearly with increasing amount of adsorbate, i.e., the process of freezing starts, probably with the formation of capillary sublimates. (III) At a certain filling fraction an abrupt rise of the shear modulus up to a plateau value is observed. This step indicates either a change in the spatial distribution of the capillary condensate or a change in its intrinsic properties. The lower the temperature, the smaller the characteristic filling fractions at which these transitions occur. During desorption a hysteresis of the shear modulus, of the attenuation, and hence of the state of the adsorbate is observed.

DOI: [10.1103/PhysRevB.78.174108](https://doi.org/10.1103/PhysRevB.78.174108)

PACS number(s): 64.70.Nd, 61.43.Gt, 62.25.-g, 64.70.D-

I. INTRODUCTION

Geometrical confinement of substances on the nanometer scale often results in altered physical properties compared to those of bulk material. For example, it is well known that the freezing point of many simple liquids adsorbed by mesoporous samples is lower than in the bulk state and that the pore condensate melts at a higher temperature than it freezes.¹⁻⁶ Numerous studies were performed to elucidate the behavior of confined liquids and their phase transition to the solid state. The techniques used are very diversified ranging from calorimetry, neutron diffraction and scattering, x-ray techniques, optical transmission, dielectric measurements, and acoustic techniques to theoretical studies.³⁻¹⁹ One of the standard systems for such investigations is mesoporous Vycor glass having a typical mean pore diameter between 7 and 10 nm. Volumetric sorption isotherms were used to record phase diagrams of argon adsorbed in Vycor glass,⁶ the characteristic quantities being temperature T , chemical potential $\Delta\mu$, and the volume filling fraction f of the pores. Freezing and melting reflect in an abrupt change in slope of $\Delta\mu(T)$, and both the freezing and the melting point increase with the filling fraction of the mesopores. But at low filling fractions, when only a few layers of argon are adsorbed on the pore walls, no liquid-solid phase transition was observed. A certain ambiguity remains since it is not easy to distinguish between small continuous or small discontinuous changes of slope $\Delta\mu(T)$. But also additional calorimetric and x-ray studies gave no indications for a phase transition, i.e., the first few layers seem to remain in an amorphous liquidlike state.^{5,6} However, an absolute clarification of how freezing proceeds in confinement has not yet been found. On the other hand molecular-dynamics simulations suggest that argon cannot crystallize at all in pores with a diameter of less than 3.4–5.1 nm.¹⁹

Ultrasonic measurements, i.e., the measurement of velocity and attenuation of propagating waves, are well suited to elucidate the behavior of confined liquids, especially with

respect to possible differences between layers adsorbed at the pore walls and capillary condensate in the pore volume. On the one hand, Page *et al.* (see Refs. 20 and 21) have used longitudinal waves to investigate the isothermal process of adsorption and desorption of liquid hexane in Vycor glass. On the other hand, Molz and co-workers (see Refs. 3, 4, and 16) used shear waves to study freezing and melting of argon and of helium in Vycor (at $f=1$, i.e., for completely filled pores). The latter method is very sensitive to changes in the aggregation state: liquids cannot sustain shear stress, i.e., the shear modulus is altered appreciably when the pore condensate freezes or melts.

We have decided to combine the advantages of both methods; i.e., in order to distinguish between wall layers and pore condensate, we study the behavior of the shear modulus during an isothermal change in pore filling (both for adsorption and desorption, and for different temperatures). The velocity of propagation, c_t , is a function of the shear modulus G of the studied medium and its density ρ , i.e., $c_t = \sqrt{G/\rho}$. In order to separate changes in density from changes in G , we have determined the actual density during filling and draining by means of simultaneous volumetric measurements of the amount of pore condensate. This allows us to evaluate G as a function of the pore filling and for various temperatures. As already mentioned, the effective shear modulus increases as soon as frozen pore condensate is present. As we shall show, this gives us some information on the process of freezing in mesopores.

II. EXPERIMENTAL

The material used to confine argon is mesoporous Vycor glass 7930 (Corning, Inc.).³⁹ Our sample has a cross section of 20×20 mm² and a height of $d=5.0$ mm. We have determined the average pore diameter from a desorption isotherm of argon at 86 K using the Kelvin equation.^{22,23} Its value is about 8 nm. In addition, the sorption isotherm yields a porosity of about 25%–26%. Before the measurements the

sample was cleaned according to the standard procedure recommended by the manufacturer.⁴⁰

We used the pulse echo method for the ultrasonic measurements.²⁴ Voltage pulses with a carrier frequency of about 12.5 MHz are generated by a Matec Pulse Modulator and Receiver (Model 6600) and converted into ultrasonic shear waves via a piezoelectric transducer that is bonded to the top surface of the sample. These propagate in the sample, are reflected at its bottom, and return to the transducer after a transit time $\Delta t = 2d/c_t$. Subsequent reflections corresponding to multiple round trips through the sample lead to a series of equidistant echoes with decreasing amplitudes. The transducer converts them back into electrical pulses and after passing the Matec Pulse Receiver they are displayed and recorded on a digital oscilloscope (LeCroy WaveSurfer™ 64Xs). The transit time through the sample, Δt , is determined from the time difference of two successive echoes, the attenuation α from the respective amplitudes, $\alpha = 20 \log_{10}(A_i/A_{i+1})/(2d)$.

As shear transducer, a LiNbO₃ crystal (41° X-cut) with chrome-gold electrodes on both sides has been bonded to the sample using an epoxy silver composite (E-Solder 3021, Von Roll USA, Inc.). This bond provides both good adhesive properties and high electrical conductivity over a broad temperature range. The incommensurability of the geometries, i.e., a cylindrical transducer with a diameter of $b = 10$ mm on top of a rectangular sample of cross section a^2 and thickness d (where $b, d \leq a/2$) helps to reduce sidewall effects that can considerably distort shape and height of the ultrasonic echoes.²⁵ Nevertheless, not only intrinsic sound absorption but also losses resulting from bonding, diffraction, as well as other effects contribute to the apparent attenuation. Therefore, the attenuation data we present in the following can only be regarded as a relative measure allowing us to monitor changes in the material properties. The particular carrier frequency of 12.5 MHz was selected because it provided the best ultrasonic signals and the lowest apparent attenuation.²⁵ The pulse width was approximately 2 μ s. In general, transit times with an absolute value between 4.5–5.5 μ s could be determined with an accuracy better than 1 ns.

Sample and bonded transducer are placed in a closed metallic container that is located on the cold head of a cryostat (Leybold Model RGD 510 closed cycle refrigerator) allowing us to stabilize its temperature T to better than ± 10 mK. Absolute values of T are measured with a precision of ± 0.25 K. The electric signal line is connected via a vacuum-sealed feedthrough. The whole cell is connected to a gas distribution system via a capillary. In this way it is possible to add or to remove a defined quantity of argon. The amount of liquid or solid argon adsorbed in the pores can be evaluated with the known volume of the gas distribution system, the temperature, the pressure before and after each filling step, and using the ideal-gas equation. So volumetric sorption isotherms are recorded, i.e., the volume filling fraction of the pores, $f = V_{\text{Ar,adsorbed}}/V_{\text{pores}}$, as a function of the vapor pressure p .^{22,23} Details of the setup are described in Ref. 26.

As the wavelength of the ultrasonic signals, about 150–180 μ m, is much larger than the average pore diameter

(8 nm), the porous sample can be regarded as homogeneous on this length scale. Consequently, the well-known relation

$$c_t = \sqrt{\frac{G}{\rho}}, \quad (1)$$

correlating the ultrasonic velocity c_t of shear waves with the (effective) density ρ of the sample and the shear modulus G , is also valid for a mesoporous sample. This velocity is given by the transit time of the signal in the sample of thickness d , $c_t = 2d/\Delta t$. The effective density,

$$\rho = \rho_0 \left(1 + \frac{nm}{M} \right), \quad (2)$$

is a function of the density of the empty sample, ρ_0 , its mass M as well as of the mass of the filled sample, $M + nm$ (here n denotes the amount of pore condensate and $m = 39.948$ g/mol its molar mass). With Eqs. (1) and (2) we obtain the ratio of the effective shear modulus G of the (partly) filled sample to the shear modulus of the empty sample G_0 ,

$$\frac{G}{G_0} = \left(\frac{\Delta t_0}{\Delta t} \right)^2 \left(1 + f \frac{n_0 m}{M} \right), \quad (3)$$

where n_0 denotes the maximum amount of pore condensate and $f = n/n_0$ is the volume filling fraction. Thus the shear modulus ratio is a function of the quantities we measure: the ultrasonic transit times of the partially filled and the empty sample, Δt and Δt_0 , and the filling fraction f .

After adding or removing a defined amount of pore condensate during a sorption measurement some time is needed to reach a stationary state (constant pressure in sample cell and gas distribution system, no changes in measured transit time and attenuation). At low filling of the sample, i.e., in the range of a few adsorbed layers, this already requires a few hours. At high f , when capillary condensate or sublimate is present, much more time is needed, in the solid regime some days, in fact. Consequently, completing an adsorption-desorption cycle is a tedious effort. At 72 K it took us about eight weeks. The reason for these long waiting times is the spatial rearrangement of pore condensate in the large sample having a complex network structure. Obviously any change in f in an adsorption or desorption step leads to a rearrangement of the condensate in the highly disordered pore network.

III. RESULTS

A. Liquid argon confined to mesopores

Bulk argon freezes at $T_f = 83.8$ K and confined argon at even lower temperatures,^{1–3,5,6} e.g., at $T_{f,\text{conf}} = 75.55$ K in Vycor.³ Before studying the freezing process, we have performed some measurements at 80 K, i.e., in the liquid regime of the pore filling. The uptake of argon becomes noticeable via a linear increase⁴¹ in the transit time with increasing amount of pore condensate [see Fig. 1(a)]. The shear modulus is displayed in Fig. 1(b). The value of G/G_0 is close to unity, the deviations being smaller than 0.5%. That is what

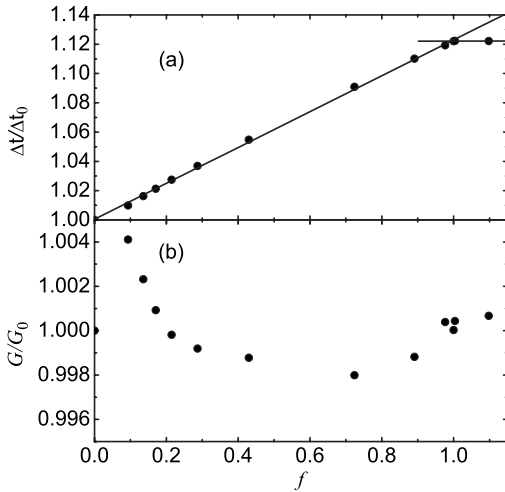


FIG. 1. (a) Ultrasonic transit time (scaled with the transit time of the unfilled sample), and (b) ratio of the effective shear modulus to the shear modulus of the empty sample upon adsorption at 80 K, i.e., above the freezing point of confined argon.

we can expect since liquids cannot sustain shear stress. Thus adsorbed argon in its liquid state does not contribute to the effective shear modulus and the data in Fig. 1(b) reflect the accuracy of the method we use.

Above the freezing point of argon, ultrasonic measurements can thus be used to evaluate sorption isotherms:²⁷ setting $G/G_0=1$ and rearranging Eq. (3) one gets the amount of the pore condensate n as a function of the ultrasonic transit times. In Fig. 2(a) we compare volumetric and ultrasonic isotherms. Once again, the good agreement reflects the accuracy of the method.

In addition, ultrasonic measurements provide some indirect information on the spatial distribution of the pore condensate. In Fig. 2(b) we display the attenuation as a function of the reduced vapor pressure p/p_0 , where p_0 denotes the vapor pressure of bulk argon. During adsorption the attenuation remains constant at about 7.5 ± 1 dB/cm, even in the range of capillary condensation (above $p/p_0 \approx 0.7$), where not only the pore walls are covered by adsorbate but the filling of the core volume starts.^{22,23} By contrast, during desorption large variations in echo amplitudes arise in the range of the desorption pressure ($p/p_0 \approx 0.74$), where the filling fraction decreases precipitously from $f \approx 1.0$ to $f \approx 0.4$.⁴² These variations go along with a deformation of the pulse shape. They probably originate from inhomogeneities in the sample that are in the range of the ultrasonic wavelength ($\lambda = 150\text{--}180$ μm at the carrier frequency of 12.5 MHz) causing multiple reflections and interference effects. Spatial inhomogeneities upon desorption have already been detected by optical transmission measurements at a wavelength of $\lambda = 632.8$ nm.¹³ Our results show that their dimensions extend at least up to length scales of the order of the acoustic wavelength.

The appearance of inhomogeneities during desorption can be explained by the irregular pore structure of the porous glass and the related formation of metastable states (e.g., by pore blocking).¹³ Since the vapor pressure depends on the local pore radius, at first larger pores are drained but only if

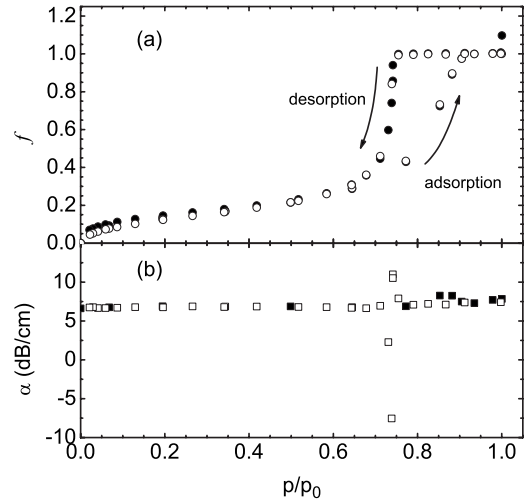


FIG. 2. (a) Comparison of sorption isotherms for argon in porous Vycor glass at 80 K determined volumetrically (closed circles) and via ultrasonic measurements (open circles). $f=n/n_0$ denotes the volume filling fraction of the pores, where n_0 is the maximum amount of pore condensate. p/p_0 is the reduced vapor pressure, i.e., the pressure normalized to that of bulk argon at 80 K. (b) Attenuation α of the ultrasonic signals as a function of the reduced vapor pressure during adsorption (closed squares) and desorption (open squares). α is measured via the amplitudes A_i of the second and the third echo, $\alpha=20 \log_{10}(A_2/A_3)/(2d)$. At the desorption pressure of $p/p_0 \approx 0.74$, where strong variations in A_2/A_3 are observed, the displayed values do not correspond to an intrinsic attenuation: the pulse shapes of the echoes are distorted due to inhomogeneities in the range of the ultrasonic wavelength.

they are not blocked by liquid remaining in smaller pores (bottlenecks). Therefore an inhomogeneous spatial distribution of empty and filled regions can form.

B. Frozen argon confined to mesopores

In Fig. 3(a) we display a volumetric sorption isotherm at $T=72$ K, i.e., more than 3 K below the freezing point of argon in Vycor and 8 K below its melting point.³ In contrast to the liquid state (Fig. 2 for $T=80$ K) the range of pore condensation upon adsorption is shifted to a higher reduced pressure (reduced adsorption pressure $p/p_0 \approx 0.96$). Below this pressure, the absorbed argon does not contribute to the effective shear modulus, i.e., $G/G_0=1$ as for a liquid [see Fig. 3(b)]. At the adsorption pressure G/G_0 increases abruptly by about 11%. Since only solids can sustain shear stress, this latter feature indicates the presence of frozen pore condensate. Likewise the attenuation increases abruptly. In contrast to what we have observed in the liquid state (see Fig. 2), the change in α does not go along with a distortion of the pulse shapes so that this feature reflects an intrinsic property of frozen argon [also temperature dependent measurements on completely filled pores ($f=1$) show an increase in α below the freezing point³¹]. On desorption a corresponding decrease in shear modulus and attenuation is observed at a desorption pressure of $p/p_0 \approx 0.74$. This hysteresis shows that frozen pore condensate remains in the pores in a range of pressure considerably larger than the corresponding one of

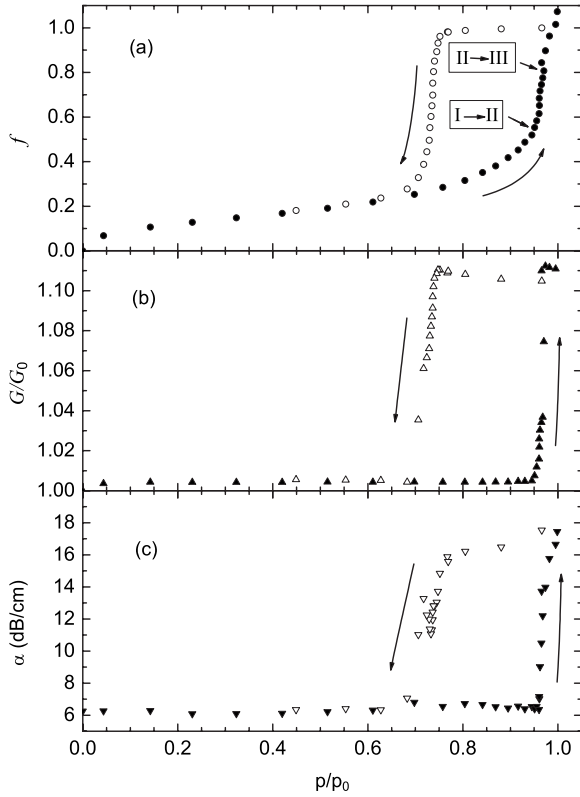


FIG. 3. (a) Filling fraction of the pores, (b) shear modulus ratio G/G_0 with $G_0=6.88$ GPa, and (c) attenuation α on adsorption (closed symbols) and desorption (open symbols) vs reduced vapor pressure at $T=72$ K. Up to the adsorption pressure of $p/p_0 \approx 0.96$ the pore condensate behaves like a liquid. Then an abrupt increase in both the shear modulus and the attenuation is observed. The arrows labeled I \rightarrow II and II \rightarrow III in (a) indicate the transition points between characteristic regions (see text and Fig. 4).

the liquid state (cf. Figs. 2 and 3). We shall discuss this point later on.

A plot of the ultrasonic transit times and of the effective shear modulus against the volumetrically determined filling fraction of the pores yields a more detailed view of the adsorption process (see Fig. 4). There are three distinct regions: at low pore fillings $G/G_0=1$ holds (region I: $0 \leq f \leq f_1$), then a linear increase is observed (region II: $f_1 \leq f \leq f_2$) followed by a jump to a plateau value (region III: $f_2 \leq f \leq 1$). In the following we are going to discuss this behavior in detail:

1. Region I

Up to a filling fraction of about 0.53 the pore condensate does not contribute to the effective shear modulus, i.e., it does not freeze at 72 K. Using an average pore radius of $r_p=4.0$ nm and a thickness of $u \approx 0.34$ nm for an adsorbed monolayer,⁴³ we can estimate the average number z of adsorbed monolayers, with the relation

$$f = \frac{V_{\text{Ar,adsorbed}}}{V_{\text{pores}}} = \frac{r_p^2 - (r_p - zu)^2}{r_p^2}. \quad (4)$$

For $f_1=0.53$ we obtain $z=3.7$, i.e., on average the first three to four adsorbed layers, corresponding to a film thick-

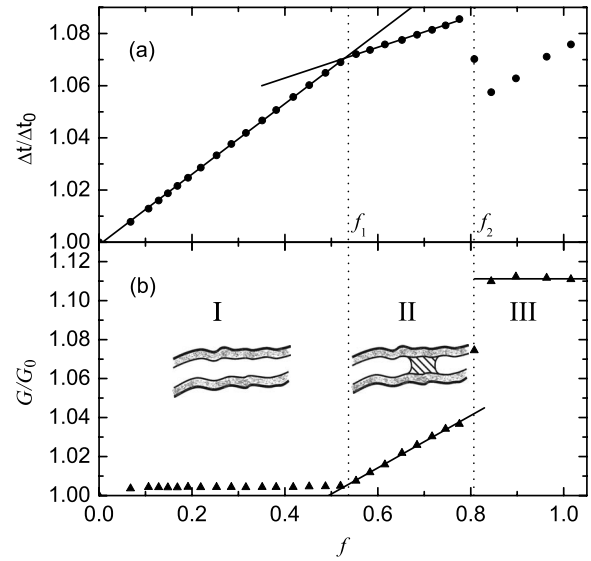


FIG. 4. (a) Ultrasonic transit time (scaled with the transit time of the unfilled sample), and (b) ratio of the effective shear modulus G to the shear modulus of the empty sample on adsorption at $T=72$ K. The process of freezing starts above a filling fraction of $f_1=0.53$. The abrupt increase in the shear modulus between regions II and III indicates a collective change in the intrinsic properties of the capillary condensate or in its spatial distribution.

ness zu of the order of 1.3 nm, do not freeze at 72 K. This result recalls what is known about argon on graphite, where the first layers remain liquid above 70 K (a single monolayer melts at about 47.2 K; in multilayer systems, the respective top layer melts at higher temperatures but still below 70 K).^{28–32}

Now let us look at the temperature dependence of region I. In Fig. 5 we display isothermal measurements of G at $T=70, 72$, and 74 K. The lower the temperature, the smaller the range of pore fillings, $[0, f_1]$, where $G/G_0=1$ holds. For $T=74$ K it extends up to $f_1=0.66$, for $T=72$ K up to f_1

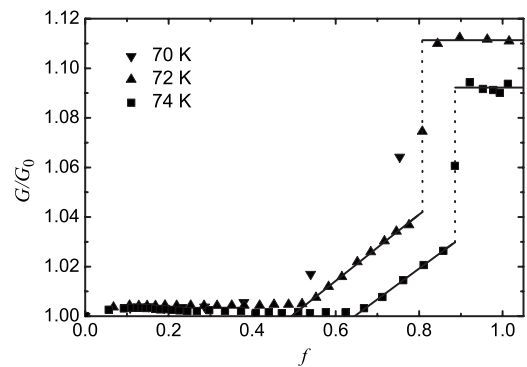


FIG. 5. Normalized effective shear modulus vs volume filling of the pores at different filling temperatures (70, 72, and 74 K). The curves shift to lower filling fractions when the temperature is reduced (regions II and III, see Fig. 4), i.e., the process of freezing ($G/G_0 > 1$) starts at lower fillings f . The shear modulus of the isotherm at 70 K could be evaluated only up to a filling fraction of about 0.75 (due to a defect of the capillary heater the gas distribution system was blocked by frozen argon).

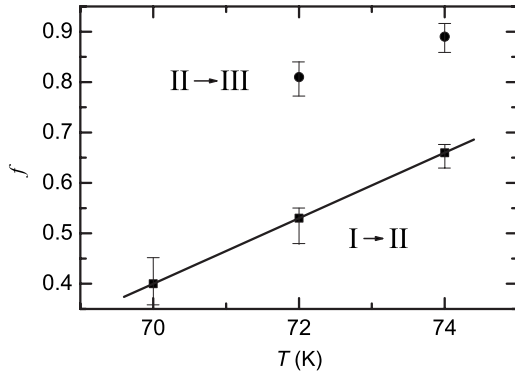


FIG. 6. Temperature dependence of the filling fraction at which the transition from region I to region II (process of freezing starts) and region II to region III was observed.

$=0.53$, and finally for $T=70$ K up to $f_1 \approx 0.4$ (see also Fig. 6). According to Eq. (4) these filling fractions correspond on average to 4.9, 3.7, and 2.7 adsorbed wall layers. Summarizing, with decreasing temperature less material remains in a liquidlike state.

Wallacher and Knorr have proposed a simple model describing thermal equilibrium in completely filled pores (see Ref. 6), where the pore walls are at first covered by “dead” layers (two monolayers) and then by a liquid shell. The latter one serves as a buffer between the frozen capillary sublimates in the pore center and the dead layers reducing the free energy of the system. There is an interplay between volume and interfacial energies and with decreasing temperature the thickness of the liquid shell decreases. According to their calculation (for a pore radius of 5 nm) at 72 K, only an amount of $f \approx 0.05$ remains liquid. Taking their model, the amount f_1 of liquidlike argon we observe would correspond to the sum of dead layers and liquid shell, which are indistinguishable in our measurements. The first two dead layers represent a filling fraction of $f_{dl}=0.33$ [cf. Eq. (4)]. Thus we get for the liquid shell $f_1 - f_{dl} = 0.33$ at 74 K and $f_1 - f_{dl} = 0.2$ at 72 K. The latter value is larger than the one predicted by the model of Wallacher and Knorr ($f \approx 0.05$), but we have to keep in mind that the total free energy they calculate depends on interfacial energies and on a coherence length, the values of which have to be estimated. Therefore, we can state at least a qualitative agreement. In the above model, the existence of liquidlike argon is an inherent thermodynamical feature of pore confined argon, i.e., it is not related to the pore size distribution of the Vycor glass. Of course, a fraction of smaller pores might contain capillary condensate that freezes at lower temperatures ($\Delta T \propto 1/r_p$, see Ref. 33). But on the other hand it would be difficult to distinguish clearly between wall layers and pore condensate in the smallest pores.

2. Region II

Now let us come back to the isothermal adsorption curve at 72 K (Fig. 4). Above $f_1=0.53$ a linear increase in the shear modulus is observed, i.e., the process of freezing starts and $G=G_0+(f-f_1)\text{const}$ holds so that $G/G_0 > 1$. Assuming that the increase is proportional to the shear modulus of frozen argon, G_{Ar} , as well as to its volume fraction, $\phi(f-f_1)$ [with

$\phi=V_{\text{pores}}/V_{\text{Vycor}}=0.25$ being the porosity of the sample] this observation can be written as

$$G(f) = G_0 + \phi(f - f_1)\alpha G_{Ar} \quad \text{for } f_1 \leq f \leq f_2. \quad (5)$$

Here α is a dimensionless constant that depends on the spatial matrix-condensate-vapor arrangement. We suppose that the freezing takes place in regions where the core volume of the pores is completely filled (formation of solid capillary sublimates). Newly added argon leads to an enlargement of these regions and thus to a linear increase in $G(f)$.

At higher temperatures region II is shifted to higher pore fillings (see Fig. 5). As already mentioned, the filling fraction f_1 that indicates the onset of the freezing process shifts from $f_1=0.53$ at 72 K to $f_1=0.66$ at 74 K. The lower the temperature, the higher the fraction of frozen argon, $f-f_1(T)$, at a given pore filling f .

In addition, the temperature dependent measurements displayed in Fig. 5 reveal another interesting feature of confined argon. Although the onset f_1 changes dramatically, the slope of the linear increase is independent of the temperature (at least for 72 and 74 K). According to Eq. (5)

$$\frac{\partial(G/G_0)}{\partial f} \propto G_{Ar} \quad (6)$$

holds for the slope. Hence the shear modulus of the confined frozen argon is not changed in this temperature range.

3. Region III

At 72 K the effective shear modulus increases abruptly at a filling fraction of $f_2=0.81$ and it remains constant at further filling [see Fig. 4(b)] although more pore condensate is taken up [see the further increase in transit time in Fig. 4(a)]. The latter observation indicates that already a solid network of filled interconnected pores governs the elastic properties, so that additional pore condensate does not lead to notable changes (i.e., percolation has already taken place, either below f_2 or at f_2). Before discussing the main experimental feature, i.e., the sudden step in G , we are going to check whether the measured plateau values are reasonable and what kind of information they reveal.

According to effective-medium theory, the measured shear modulus G of a heterogeneous material depends on both the material parameters as well as on the spatial distribution, i.e., on the microstructure. This makes it difficult to evaluate precisely the shear modulus of the confined frozen argon. But at least we can get an estimate since there are lower and upper bounds for G corresponding to the principles of least work and of minimum potential energy, respectively.³⁴ For a two-phase system of arbitrary microstructure the upper bound is given by $G \leq \sum_i (V_i/V) G_i$, i.e., each component i contributes at maximum with its volume fraction. For the lower bound the volume-weighted reciprocal values are to be taken, i.e., $G \geq 1 / \{ \sum_i (V_i/V) / G_i \}$ holds. We use this lower bound at $f=1$, where we have to consider only the shear modulus of quartz, $G_Q=27.9$ GPa,³⁵ and that of the pore filling. With $G(f=1)=1.11G_0=7.64$ GPa at 72 K and a porosity $\phi=0.25$ we obtain

$$(G_{\text{Ar}})_{f=1} \leq \frac{\phi}{\frac{1}{G} - \frac{1-\phi}{G_0}} = 2.4 \text{ GPa}. \quad (7)$$

Here G_{Ar} denotes the shear modulus of the whole pore filling, i.e., of pore condensate and wall layers. The wall layers do not contribute at low filling fractions $f \leq f_1$, where they have a free surface facing the empty core volume. But when pore sublimate forms they become interfacial layers between two solids, i.e., between matrix and frozen argon, and thus their properties might change (at least they are able to transmit elastic vibrations). Therefore, Eq. (7) only yields an upper bound for the shear modulus of the pore filling as a whole but it does not allow us to separate contributions from pore sublimate and wall layers. We can compare this result to what is known from literature: depending on the direction of wave propagation, single crystals of argon exhibit a shear modulus between 0.4 and 1.2 GPa at temperatures from 80 to 82 K (see the values for $(C_{11} - C_{12})/2$ and for C_{44} in Table III of Ref. 36 as well as the references cited therein). For polycrystalline argon a value of $G_{\text{Ar,poly}} \approx 0.9$ GPa has been reported.³⁷ Thus our effective-medium analysis is in good agreement with this data showing that the confined frozen argon can be in a crystalline or in a polycrystalline state.

Now let us come back to the main experimental feature, i.e., the sudden increase in the effective shear modulus G at f_2 . The value of f_2 shifts to lower fractions at reduced temperature (see Figs. 5 and 6). Let δ be an infinitesimal filling fraction so that $G(f_2 - \delta)$ denotes the shear modulus just before the step (in region II) and G_{plateau} the plateau value of the shear modulus at $f > f_2$ (in region III). Both quantities increase with decreasing temperature (see Fig. 5) and so does their difference, the height of the step $G_{\text{plateau}} - G(f_2 - \delta)$ increases when the temperature is lowered from 74 to 72 K. We do not think that the step in G is due to a sudden freezing of the wall layers we observe in region I: their filling fraction f_1 shows the opposite behavior, i.e., the lower the temperature, the lower f_1 . But there is another correlation to note. As already discussed above [see Eq. (5)]

$$(G_{f_2-\delta} - G_0) \propto (f_2 - f_1) \quad (8)$$

holds before the step (region II). Interestingly, a similar relation seems to hold at least approximately for the difference between the effective (measured) plateau value at high f and the matrix value at low f , when no frozen argon is present

$$(G_{\text{plateau}} - G_0) \propto (f_2 - f_1). \quad (9)$$

When the temperature is lowered from 74 to 72 K, this difference in G increases by 22% from 0.09 to 0.11 (see Fig. 5). The amount of frozen capillary sublimate before the step changes from $f_2 - f_1 \approx 0.89 - 0.66 = 0.23$ to $f_2 - f_1 \approx 0.81 - 0.53 = 0.28$, i.e., it also increases by 22% (see Fig. 6). So at least in our restricted range of temperature, Eq. (9) is a good approximation. Summarizing, the total increase in the shear modulus G upon filling, $G_{\text{plateau}} - G_0$, seems to be correlated with the amount of frozen capillary sublimate before the step: $f_2 - f_1$ increases with decreasing temperature and so does $G_{\text{plateau}} - G_0$. The sudden increase at f_2 suggests a col-

lective effect and in what follows we shall discuss some possible mechanisms. It is clear that either the spatial distribution of the pore condensate changes or its intrinsic properties.

On the one hand percolation, i.e., a collective cross linking of existing regions of capillary sublimate might lead to a change in the effective elastic properties. The observation that the shear modulus is constant above f_2 indicates that already a solid network of filled interconnected pores governs the elastic properties, so that additional pore condensate does not lead to notable changes (i.e., percolation has already taken place, either below f_2 or at f_2). But the transition between region II and region III takes place rather late, at $f_2 \approx 0.8 - 0.9$, when the porous Vycor is nearly completely filled (see also Fig. 3). Thus already below f_2 percolating paths may exist. In addition, f_2 would be a temperature dependent percolation threshold.

On the other hand, not the spatial distribution of the capillary condensate but a change in its intrinsic properties, i.e., of G_{Ar} might lead to the observed step of the measured effective G . One possibility would be a structural change. The authors of Ref. 12 report on x-ray diffraction measurements on mesoporous samples, where the onset of crystallization is observed at similar high filling fractions. If this onset coincides with f_1 , capillary sublimate is always (poly-) crystalline; if it coincides with f_2 , there would be a transition from an amorphous to a (poly-)crystalline state. In order to check this, x-ray measurements on our samples are needed. We conclude with a last possibility. The authors of Ref. 11 have observed an upward shift of the melting and freezing temperatures at very high filling fractions (for argon in SBA-15 mesoporous silica). They have explained this effect by a tensile pressure release upon reaching bulk-vapor coexistence: the pore condensate exhibits concave menisci and is thus under a negative hydrostatic pressure of the order of 100 bar. At high fillings, when it reaches the tapered pore mouths the curvature radius and consequently the tensile pressure in the pore condensate is reduced. Since our f_2 values correspond to very high reduced vapor pressures (see Fig. 3 for $T=72$ K), we can imagine a similar situation: the release of tensile pressure might lead to a tightening of the pore condensate so that G_{Ar} increases. But also another phenomenon can give rise to a sudden change of pressure: Günther *et al.*³⁸ have recently observed an abrupt contraction of pore walls at capillary condensation, probably due to attractive interactions between condensate and walls.

4. Desorption hysteresis

Finally, we want to discuss briefly the hysteresis upon desorption (see the isotherm at $T=72$ K in Fig. 3). An abrupt decrease in the shear modulus is observed at the desorption pressure of about $p/p_0 \approx 0.74$. Also the attenuation decreases abruptly at this pressure. Again a plot against the filling fraction yields more information (see Fig. 7). At the beginning of the desorption process ($0.9 \leq f \leq 1$) the attenuation decreases but the shear modulus remains constant, probably because only a few pores are partially drained, a process that does not affect the elastic properties of the whole frozen pore network. Between $f=0.9$ and $f=0.39$ the shear modulus de-

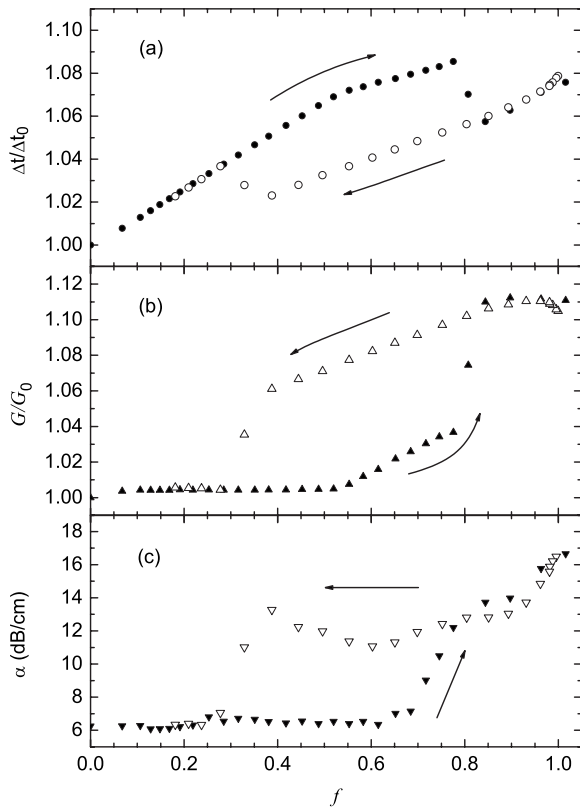


FIG. 7. (a) The ultrasonic transit time, (b) the effective shear modulus, and (c) the attenuation show a hysteresis between adsorption and desorption (measurement at $T=72$ K). From this behavior one can infer that during desorption the pore condensate is solid above a filling fraction of 0.33, whereas during adsorption solid regions appear only at a higher filling fraction (>0.53).

creases linearly, indicating that little by little the number of filled pores is reduced. Between a filling fraction of $f=0.39$ and $f=0.29$ both the attenuation and the shear modulus drop precipitously and reach the respective values for Vycor glass. In this range the remaining network of interconnected pores finally breaks down. Below $f=0.29$ only liquidlike argon, i.e., wall layers or capillary condensate in very small pores, is present. There are two main differences between adsorption and desorption. During desorption frozen capillary condensate is present in a larger range of filling fractions (between $f=0.29$ and $f=1$) than in adsorption (between $f=0.53$ and $f=1$). In addition, during desorption higher values of shear modulus and attenuation are observed in the range from $f=0.29$ to $f=0.8$.

Remember that the measured effective properties, shear modulus, and attenuation reflect both the properties of argon as well as its spatial distribution. Therefore, pore blocking, where small bottlenecks filled with argon prevent the draining of bigger pores, can explain the above findings. In this case at first freely accessible larger pores are drained. For this reason, at a given filling fraction $f \in [0.29, 0.8]$ there is

more frozen argon during desorption than during adsorption and the spatial distribution differs.

IV. CONCLUSIONS

The combination of volumetric and ultrasonic measurements permits the determination of the effective elastic properties of a porous sample as a function of the filling fraction. The measurements of adsorption isotherms below the freezing point of argon yielded a systematic behavior, showing three distinct ranges. The first few adsorbed layers do not contribute to the effective shear modulus G , i.e., they remain in a liquidlike state (region I). G increases linearly when capillary sublimate forms (region II). Finally, the shear modulus increases abruptly up to a plateau value (region III). The lower the temperature, the lower the characteristic filling fractions at which the transitions between these regions occur. In addition a hysteresis of the elastic properties of the pore condensate was observed reflecting pore blocking effects. In particular, the adsorption isotherms revealed some interesting features:

(i) The first liquidlike fraction of argon in the range $[0, f_1]$ seems to remain liquid during an isotherm, i.e., there is no indication that a further filling of the pores would lead to a phase transition. The total increase in the shear modulus upon a complete filling of the pores, $G_{\text{plateau}} - G_0$, is not correlated with the amount f_1 of liquidlike argon at lower fillings, but is proportional to $f_2 - f_1$, i.e., to the amount of frozen argon in region II.

(ii) The amount of frozen argon in region II, $f_2 - f_1$, increases markedly with decreasing temperature, although the temperature variation is small, $\Delta T=2$ K. But the slope $\partial G / \partial f$ and thus G_{Ar} is approximately independent of temperature [see Eq. (6)].

(iii) The total amount of liquidlike argon, f_1 , decreases with decreasing temperature. In other words, the lower the temperature, the more frozen argon is present at complete pore fillings, $f=1$. The freezing of pore-confined argon over a range of temperatures is the main reason for the increase in $G(f=1)$ with decreasing temperature, although we cannot exclude an additional intrinsic temperature dependence of G_{Ar} due to stress relaxation (thermally activated motion of vacancies) as proposed by Molz *et al.* (see Ref. 3).

The most prominent experimental feature in this work is the observation of the sudden increase in G at the transition from regions II to III. This seems to be a collective effect, i.e., either the spatial distribution of the capillary condensate or its intrinsic elastic properties change.

ACKNOWLEDGMENTS

We are grateful to W. Arnold and H. Schmitt (Universität des Saarlandes) for much practical advice regarding ultrasonic experiments, as well as to K. Knorr (Universität des Saarlandes) for attracting our attention to this field of research and for helpful discussions.

*k.schappert@mx.uni-saarland.de

†rolf.pelster@mx.uni-saarland.de

- ¹H. K. Christenson, *J. Phys.:* Condens. Matter **13**, R95 (2001).
- ²G. Litvan, *Can. J. Chem.* **44**, 2617 (1966).
- ³E. Molz, A. P. Y. Wong, M. H. W. Chan, and J. R. Beamish, *Phys. Rev. B* **48**, 5741 (1993).
- ⁴E. B. Molz and J. R. Beamish, *J. Low Temp. Phys.* **101**, 1055 (1995).
- ⁵P. Huber and K. Knorr, *Phys. Rev. B* **60**, 12657 (1999).
- ⁶D. Wallacher and K. Knorr, *Phys. Rev. B* **63**, 104202 (2001).
- ⁷K. M. Unruh, T. E. Huber, and C. A. Huber, *Phys. Rev. B* **48**, 9021 (1993).
- ⁸Y. Wang, W. Snow, and P. Sokol, *J. Low Temp. Phys.* **101**, 929 (1995).
- ⁹M.-C. Bellissent-Funel, J. Lal, and L. Bosio, *J. Chem. Phys.* **98**, 4246 (1993).
- ¹⁰D. Wallacher, R. Ackermann, P. Huber, M. Enderle, and K. Knorr, *Phys. Rev. B* **64**, 184203 (2001).
- ¹¹C. Schaefer, T. Hofmann, D. Wallacher, P. Huber, and K. Knorr, *Phys. Rev. Lett.* **100**, 175701 (2008).
- ¹²T. Hofmann, D. Wallacher, P. Huber, and K. Knorr, *J. Low Temp. Phys.* **140**, 91 (2005).
- ¹³D. Wallacher, V. P. Soprunyuk, A. V. Kityk, P. Huber, and K. Knorr, *Phys. Rev. B* **71**, 052101 (2005).
- ¹⁴V. P. Soprunyuk, D. Wallacher, P. Huber, K. Knorr, and A. V. Kityk, *Phys. Rev. B* **67**, 144105 (2003).
- ¹⁵D. Wallacher, V. P. Soprunyuk, K. Knorr, and A. V. Kityk, *Phys. Rev. B* **69**, 134207 (2004).
- ¹⁶J. R. Beamish, A. Hikata, L. Tell, and C. Elbaum, *Phys. Rev. Lett.* **50**, 425 (1983).
- ¹⁷B. Borisov, E. Charnaya, T. Loeser, D. Michel, C. Tien, C. Wur, and Y. A. Kumzerov, *J. Phys.:* Condens. Matter **11**, 10259 (1999).
- ¹⁸B. F. Borisov, E. V. Charnaya, P. G. Plotnikov, W.-D. Hoffmann, D. Michel, Y. A. Kumzerov, C. Tien, and C.-S. Wur, *Phys. Rev. B* **58**, 5329 (1998).
- ¹⁹K. Nishio, W. Shinoda, T. Morishita, and M. Mikami, *J. Chem. Phys.* **122**, 124715 (2005).
- ²⁰J. H. Page, J. Liu, B. Abeles, H. W. Deckman, and D. A. Weitz, *Phys. Rev. Lett.* **71**, 1216 (1993).
- ²¹J. H. Page, J. Liu, B. Abeles, E. Herbolzheimer, H. W. Deckman, and D. A. Weitz, *Phys. Rev. E* **52**, 2763 (1995).
- ²²S. Gregg and K. Sing, *Adsorption, Surface Area, and Porosity* (Academic, London, 1982).
- ²³F. Rouquerol, J. Rouquerol, and K. Sing, *Adsorption by Powders and Porous Solids* (Academic, London, 1999).
- ²⁴R. Truell, C. Elbaum, and B. B. Chick, *Ultrasonic Methods in Solid State Physics* (Academic, New York, 1969).
- ²⁵E. P. Papadakis, in *Ultrasonic Measurement Methods*, Physical Acoustics Vol. XIX, edited by R. N. Thurston and A. D. Pierce (Academic, San Diego, 1990), pp. 81–155.
- ²⁶K. Schappert, Diplomarbeit, Universität des Saarlandes, 2007.
- ²⁷K. Warner and J. Beamish, *J. Appl. Phys.* **63**, 4372 (1988).
- ²⁸A. D. Migone, Z. R. Li, and M. H. W. Chan, *Phys. Rev. Lett.* **53**, 810 (1984).
- ²⁹P. Day, M. Lysek, M. LaMadrid, and D. Goodstein, *Phys. Rev. B* **47**, 10716 (1993).
- ³⁰H. S. Youn and G. B. Hess, *Phys. Rev. Lett.* **64**, 918 (1990).
- ³¹J. M. Phillips, Q. M. Zhang, and J. Z. Larese, *Phys. Rev. Lett.* **71**, 2971 (1993).
- ³²G. B. Hess, in *Phase Transitions in Surface Films II*, NATO Advanced Studies Institute, Series B: Physics, edited by H. Taub, G. Torzo, H. Lauter, and J. S. C. Fain (Plenum, New York, London, 1990), Vol. 267, pp. 357–389.
- ³³J. Warnock, D. D. Awschalom, and M. W. Shafer, *Phys. Rev. Lett.* **57**, 1753 (1986).
- ³⁴B. Paul, *Trans. Metall. Soc. AIME* **218**, 36 (1960).
- ³⁵Data sheet for Base Vycor 7913, Corning, Inc.
- ³⁶Y. Fujii, N. A. Lurie, R. Pynn, and G. Shirane, *Phys. Rev. B* **10**, 3647 (1974).
- ³⁷J. R. Barker and E. R. Dobbs, *Philos. Mag.* **46**, 1069 (1955).
- ³⁸G. Günther, J. Prass, O. Paris, and M. Schoen, *Phys. Rev. Lett.* **101**, 086104 (2008).
- ³⁹The Vycor glass 7930 (Corning, Inc.) used is similar to that in Refs. 6, 10, 14, and 15, where the mean diameter of the respective batches varies between 7 and 10 nm.
- ⁴⁰After evacuating the sample it was put into 30% hydrogen peroxide. Then it was heated at about 100 °C for several hours. Thereafter it was washed several times in de-ionized water and finally inserted into the sample cell.
- ⁴¹A Taylor expansion of Eq. (3) yields $\frac{\Delta t}{\Delta t_0} = \sqrt{\frac{\rho}{\rho_0}} = \sqrt{1 + f \frac{m_0 m}{M}} \approx 1 + (\frac{1}{2} \frac{m_0 m}{M}) f$.
- ⁴²A similar effect has also been observed for the attenuation of longitudinal sound waves propagating in Vycor glass filled with liquid hexane, see Refs. 20 and 21.
- ⁴³The thickness u of an adsorbed monolayer was estimated using the density of argon, $\rho_{Ar} = 1.66 \text{ g/cm}^3$ at $T = 72 \text{ K}$, its molar mass, $m = 39.948 \text{ g/mol}$, and the Avogadro constant N_A : $u \approx [m / (\rho N_A)]^{1/3} = 0.34 \text{ nm}$.